

Alpha-decay properties of superheavy elements $Z = 113 - 125$ in the relativistic mean-field theory with vector self-coupling of ω meson

M.M. Sharma and A.R. Farhan

Physics Department, Kuwait University, Kuwait 13060

G. Münzenberg

Gesellschaft für Schwerionenforschung, Planckstrasse 1, D-64220, Darmstadt, Germany

(Dated: November 11, 2018)

We have investigated properties of α -decay chains of recently produced superheavy elements $Z = 115$ and $Z = 113$ using the new Lagrangian model NL-SV1 with inclusion of the vector self-coupling of ω meson in the framework of the relativistic mean-field theory. It is shown that the experimentally observed alpha-decay energies and half-lives are reproduced well by this Lagrangian model. Further calculations for the heavier elements with $Z=117-125$ show that these nuclei are superdeformed with a prolate shape in the ground state. A superdeformed shell-closure at $Z = 118$ lends an additional binding and an extra stability to nuclei in this region. Consequently, it is predicted that the corresponding Q_α values provide α -decay half-lives for heavier superheavy nuclei within the experimentally feasible conditions. The results are compared with those of macroscopic-microscopic approaches. A perspective of the difference in shell effects amongst various approaches is presented and its consequences on superheavy nuclei are discussed.

PACS numbers: 21.60.-n, 21.30.Fe, 27.90.+b, 23.60.+e

I. INTRODUCTION

The large progress in superheavy element research has delivered challenging experimental data. This provides nuclear structure theory an opportunity to interpret the new experimental results and to improvise on predictions for the location of the superheavy nuclei on the basis of the new experimental data. At present there exist two sets of data due to two methods employed for superheavy-element synthesis[1].

The heaviest elements known today, the elements with $Z = 110$, 111, and 112, have been produced by cold fusion of heavy ions. Targets of ^{208}Pb or ^{209}Bi were irradiated with the appropriate projectiles ^{64}Ni or ^{70}Zn to produce the isotopes $^{271}110$, $^{272}111$, and $^{277}112$ [2, 3]. These have been identified by long α decay chains leading to known isotopes. These data are on a safer ground, for they have been verified in different laboratories[4, 5]. Recently, even the heaviest species in this series, $^{277}112$, has been confirmed independently [3, 6]. The important new result of these experiments is the discovery of a region of deformed, shell stabilized nuclei [7], centered at $Z = 108$ (Hassium) and $N = 162$. Theoretical calculations have argued that these nuclei are stabilized due to a hexadecapole deformation in the ground state[8, 9, 10].

The second approach to synthesize heavy elements leads to elements with $Z = 114$, 115, and 116. Beams of ^{48}Ca on actinide targets e.g. ^{244}Pu and $^{245,248}\text{Cm}$ were used. The isotopes of $^{286-289}114$, and $^{290-293}116$ have been identified in various experiments [11, 12, 13, 14]. Recently, the isotopes $^{287,288}115$ have been observed in irradiations of ^{243}Am target with ^{48}Ca beam [15]. These results are exciting and of special attraction for theory as the new region is located already close to the expected superheavy nuclei. The experimental problem is that the

observed nuclides decay over long α -decay chains ending in spontaneous fission. These form an island of nuclei in itself and cannot be connected to the known region of isotopes. This makes an unambiguous identification with the presently used parent-daughter method impossible. To cope with this problem, a number of consistency checks have been made [14]. In addition, first promising experiments to verify the chemical nature of these elements are underway [16].

Experimental investigations of superheavy elements encounter a general problem that only a few atomic nuclei of each species are produced. Presently, for the heaviest species only basic properties can be directly extracted from experiment. These are Q_α -values and lifetimes. Most of the known nuclides have odd proton or neutron numbers and are not likely to decay by ground state transitions. Moreover, superheavy nuclei have a complicated level structure with high spin and low spin states being close together. They are likely to form isomers [1]. This makes a comparison with theoretical predictions a little difficult. In those cases where the chains end in fission, Q_α -values and lifetimes are the only experimental information that can be extracted for nuclides along the chain. However, ground state masses of nuclei cannot be obtained.

Properties and structure of superheavy nuclei have been investigated extensively using various approaches. The approaches consist of microscopic nature such as non-relativistic density-dependent Skyrme Hartree-Fock (SHF) theory and the Relativistic Mean-Field (RMF) theory or macroscopic-microscopic type. In the latter category, total binding energy of nuclei is obtained as a sum of a smooth energy based upon liquid drop type formula on which shell correction is imposed using the method of Strutinsky [17, 18]. The most notable effort in

this direction has been the Finite-Range Droplet Model (FRDM) [19]. The shell correction energies were calculated in the FRDM in order to identify major magic numbers in the region of superheavy nuclei. The FRDM predicts a major proton magic number at $Z = 114$ beyond the well known magic number $Z = 82$. Experimental data, however, give little support to this magic number. Calculations using the macroscopic-microscopic approach have also been performed by another group [20, 21, 22, 23], where Yukawa-plus-exponential model has been used for the macroscopic component and the Strutinsky shell correction is used for the microscopic component. Calculations of properties of superheavy nuclei have been rather successful in the macroscopic-microscopic approaches.

Extensive studies of superheavy nuclei have also been performed within self-consistent mean-field models of SHF type [24] or comparative studies of SHF models and RMF models [25, 26, 27, 28, 29] have been done. One of the first studies of the properties of superheavy nuclei within the RMF theory was performed earlier in ref. [30] using the force NL-SH [31]. It was shown that neutron number $N = 184$ appears to be magic for lighter superheavy nuclei, whereas it diminishes for heavier superheavies for $Z > 114$. In this work shell correction energies were also calculated for heaviest deformed superheavy nuclei. For the proton number, there was an indication of a deformed shell closure at $Z = 114$. This was consistent with the predictions of the FRDM for a strong shell gap at $Z = 114$ in the deformed region.

In order to identify magic numbers in the region of superheavy elements theoretically, extensive shell correction calculations have been performed by Kruppa et al. [32] for a set of the Skyrme and RMF forces. It is shown that Skyrme models predict the strongest shell effects at $N = 184$ and $Z = 124, 126$, but not at $Z = 114$. On the other hand, several RMF forces considered in this work [32] do not show a shell gap $N = 184$. This contrasting difference in the behavior of magic numbers between the Skyrme forces and RMF forces can be attributed to the difference in the shell structure in the RMF and SHF approaches. This derives partly from the difference in the spin-orbit interaction and its isospin dependence. It was shown in ref. [33] that isospin dependence in the Skyrme Hartree-Fock theory is different than that in the RMF theory. This difference in the isospin dependence of the spin-orbit potential was shown to be responsible for a correct description of anomalous isotope shifts in Pb isotopes [33]. A modification in the isospin dependence of the spin-orbit potential [33, 34] in the Skyrme Ansatz allowed a proper description of the isotope shifts in Pb nuclei, though refs. [33] and [34] provide for different prescriptions for the dependence. It is, therefore, expected that Skyrme forces without such a modification would yield results different than those from the RMF forces.

A significant difference between the RMF theory and SHF theory has emerged in a systematic study of fission

barriers of actinide nuclei. A comparative study of fission barriers has been performed recently in SHF models and RMF theory [35]. It has been shown that the RMF forces considered in this work predict lower fission barriers than most of the SHF models. It is, however, not clear whether this discrepancy holds for all the available RMF forces. This difference between RMF and SHF forces, if it holds in general, needs to be understood. It is surmised that this difference may lie in the difference in shell structure between the two theories.

We have studied the recent α -decay chains of $Z = 115$ [15] employing the RMF theory in the present paper. As it is well established, the Relativistic Mean-Field (RMF) theory [36] has proved to be successful in providing a framework for description of various facets of nuclear properties [31, 37, 38, 39, 40, 41]. The relativistic Lorentz covariance of the theory allows an intrinsic spin-orbit interaction based upon exchange of σ - and ω -mesons. This has been shown to be advantageous for properties such as anomalous isotope shifts in Pb nuclei [42]. The RMF theory has achieved significant success in respect of nuclei near the stability line as well as for nuclei far away from the stability line [31, 38, 40]. The nonlinear scalar self-coupling of σ -meson has been the most successful model in the RMF theory used so far. However, a closer analysis of Lagrangians with the non-linear scalar coupling of σ -meson has shown [43] that shell effects with these model Lagrangians at the stability line are stronger than the experimental data. This effect is extended to regions far beyond the stability line. It has been shown that the nature of the shell effects along the stability line does in turn influence the shell effects in the extreme and unknown regions [44].

In the present paper, we have calculated properties of α -decay chains of the newly discovered superheavy nuclei $^{288}115$ and $^{287}115$ [15] using the Lagrangian model of the vector self-coupling of ω meson. In Section II, we present a perspective of the shell effects with a view to show a relationship of the shell effects in the r-process region to those in the superheavy region. We allude briefly to some of the distinctive features of the RMF theory in Section II. We will also refer to some of these features in our discussion. A brief formalism of the RMF theory is presented in Section III, and details of RMF calculations are provided in Section IV. Section V discusses results of the RMF calculations on Q_α values, α -decay half-lives and deformation properties. A comparison of the results on Q_α values and α -decay half-lives is made with some earlier calculations and also with predictions made by some macroscopic-microscopic models. We also predict properties of heavier superheavy nuclei which can be α -decay precursors of the nuclei $^{288}115$ and $^{287}115$. Deformed single-particle spectra are presented in order to visualize existence of possible islands of stability in the deformed region. The last section summarizes the results in view of experimental feasibility of synthesis of heavier superheavy nuclei.

II. IMPORTANCE OF THE SHELL EFFECTS

The spin-orbit interaction and consequently how the shell effects behave in the extreme regions plays a significant role in carving out shell gaps in superheavy nuclei and in nuclei near r-process path. In this respect, the RMF theory has an inherent advantage in that the spin-orbit interaction arises naturally as a result of the Lorentz-Dirac structure of nucleons. Consequently, the RMF theory has shown an immense potential in being able to describe properties of nuclei along the stability line and also for a large number of nuclei beyond the stability line.

Recently, it was shown [43] that Lagrangian models with the non-linear scalar coupling of σ meson only overestimate the shell effects at the stability line. In order to remedy the problem of strong shell effects, the nonlinear vector self-coupling of ω meson was introduced in Ref. [43]. It was shown [43] that the ensuing Lagrangian parameter set NL-SV1 is able to reproduce the shell effects in Ni and Sn isotopes near the stability line. It was also shown [44] that the force NL-SV1 based upon the vector self-coupling of ω -meson is also successful in describing the available data on the shell effects across the waiting-point nucleus ^{80}Zn . This exemplifies the importance of an appropriate description of the shell effects along the line of stability with a view to be able to extrapolate the shell effects in the extreme regions such as near the r-process path. Due to this reason, we consider that a description of superheavy nuclei in the extreme regions can be put on a footing similar to that of nuclei which are close to the r-process path.

III. RELATIVISTIC MEAN-FIELD THEORY

The RMF approach [36] is based upon the Lagrangian density which consists of fields due to the various mesons interacting with nucleons. The mesons include the isoscalar scalar σ -meson, the isovector vector ω -meson and the isovector vector ρ -meson. The Lagrangian density is given by:

$$\begin{aligned} \mathcal{L} = & \bar{\psi} \left(\not{p} - g_\omega \not{\omega} - g_\rho \not{\rho} - \frac{1}{2} e(1 - \tau_3) \not{A} - g_\sigma \not{\sigma} - M \right) \psi \\ & + \frac{1}{2} \partial_\mu \sigma \partial^\mu \sigma - U(\sigma) - \frac{1}{4} \Omega_{\mu\nu} \Omega^{\mu\nu} + \frac{1}{2} m_\omega^2 \omega_\mu \omega^\mu \\ & + \frac{1}{2} g_4 (\omega_\mu \omega^\mu)^2 - \frac{1}{4} \mathbf{R}_{\mu\nu} \mathbf{R}^{\mu\nu} + \frac{1}{2} m_\rho^2 \rho_\mu \rho^\mu - \frac{1}{4} F_{\mu\nu} F^{\mu\nu} \end{aligned} \quad (1)$$

The bold-faced letters indicate the vector quantities. Here M , m_σ , m_ω and m_ρ denote the nucleon-, the σ -, the ω - and the ρ -meson masses respectively, whereas g_σ , g_ω , g_ρ and $e^2/4\pi = 1/137$ are the corresponding coupling constants for the mesons and the photon, respectively.

The nonlinear scalar interaction has been used extensively to describe the ground-state properties of finite nuclei. Herein, the σ meson is assumed to move in a

TABLE I: The Lagrangian parameters of the force NL-SV1 used in the calculations. All the masses are in MeV. While g_2 is in fm^{-1} , all the other coupling constants are dimensionless. Here g_4 represents the quartic coupling of ω meson.

$M = 939.0$	$g_\sigma = 10.1248$	$g_2 = -9.2406$
$m_\sigma = 510.0349$	$g_\omega = 12.7266$	$g_3 = -15.388$
$m_\omega = 783.0$	$g_\rho = 4.4920$	$g_4 = 41.0102$
$m_\rho = 763.0$		

scalar potential of the form:

$$U(\sigma) = \frac{1}{2} m_\sigma^2 \sigma^2 + \frac{1}{3} g_2 \sigma^3 + \frac{1}{4} g_3 \sigma^4. \quad (2)$$

where g_2 and g_3 represent the parameters of the nonlinear coupling of σ meson to nucleon. This model Lagrangian has been very successful in describing properties of nuclei at the stability line and also for nuclei away from the stability line. The coupling constant for the non-linear ω -term is denoted by g_4 in the Lagrangian of Eq. (1). The vector self-coupling of the ω -meson was first proposed in ref. [46], where properties of nuclear matter associated to this potential were discussed. It is interesting to note that introduction of the non-linear coupling of ω -meson softens the equation of state (EOS) of the nuclear matter significantly. This has the consequence that the maximum neutron star mass with such an EOS appears within the bounds of empirically observed values.

IV. DETAILS OF THE CALCULATIONS

The RMF calculations in this work have been performed in an axially symmetric deformed basis. The method of expansion [38] of wavefunctions into harmonic-oscillator basis has been used to solve the Dirac and Klein-Gordan equations. Both the fermionic and bosonic fields have been expanded in a harmonic oscillator basis of 20 shells. The pairing has been included within the BCS scheme employing constant pairing gaps. The prescription of ref. [47] which provides for a best fit of pairing gaps for neutrons and protons over a large range of nuclei has been used. Accordingly, pairing gaps are taken as

$$\Delta_{n(p)} = 4.8 N^{-1/3} (Z^{-1/3}) \quad (3)$$

where N and Z represent the neutron and proton number of a nucleus. The Lagrangian parameter set NL-SV1 [43] has been used for all the calculations. The parameters of the force NL-SV1 are presented in Table I. In this work, we have not included the blocking of pairing for an odd particle. Extensive calculations with the blocking of pairing would be presented elsewhere.

We have carried out constrained calculations with a quadratic constraint. The potential energy landscapes of nuclei over a large range of quadrupole deformation

have been mapped out and various possible minima in the total energy have been identified. This also serves to confirm the total binding energy of ground state as obtained in individual RMF+BCS minimizations.

V. RESULTS AND DISCUSSION

A. Q_α values and half-lives

The decay chain of the superheavy nucleus $^{288}\text{115}$ ($Z=115$) was observed [15] for 3 events in the $3n$ evaporation channel in the reaction $^{243}\text{Am} + ^{48}\text{Ca}$ with the projectile energy $E = 248$ MeV. The energy of alpha particles emitted as a result of consecutive α -decay of various product nuclei is within about 250 keV in the three events. The maximum dispersion in the alpha energy has been observed for $^{284}\text{113}$ amounting to about 0.5 MeV. The best two values agreeing with each other have been selected as the acceptable value for Q_α in ref. [15].

Results of the RMF calculations with the Lagrangian set NL-SV1 for the newly discovered chains of superheavy nuclei are shown in Figs. 1 and 2. Figure 1 shows the difference ΔQ_α of the calculated Q_α values from the experimentally obtained ones for the chain with the parent nucleus $^{288}\text{115}$. For the nucleus $^{288}\text{115}$, calculations with NL-SV1 show a deviation from the experimental value by about 0.8 MeV. For the nuclei $^{284}\text{113}$ and $^{280}\text{111}$, NL-SV1 shows a very good agreement with the data. On going to lighter products of the chain, i.e. for ^{276}Mt ($Z=109$) and ^{272}Bh ($Z=107$), our results agree with the data within about half an MeV. A comparison is also made with the relativistic mean-field calculations of ref. [48] using the parameter set TMA [49]. Results of TMA with the use of constant pairing (open square) and a density-dependent δ -pairing force (diamonds) are shown. The results shown with the δ -pairing also include the blocking effect. The Q_α obtained with the constant pairing for the nucleus $^{288}\text{115}$ is about the same as that with NL-SV1. However, for other nuclei such as $^{284}\text{113}$ and ^{272}Bh ($Z=107$) the disagreements with the data amounts to about 1 MeV. Whilst for $^{284}\text{113}$, TMA with constant pairing overestimates the experimental value by about 1 MeV, it underestimates the experimental Q_α for ^{272}Bh ($Z=107$) by about the same amount. In comparison, the use of the δ -pairing force with the blocking has shown some improvements in the results with TMA. It is seen from the figure that our present calculations with NL-SV1 are in good agreement with the Q_α values of the decay chain of $^{288}\text{115}$ with the exception for the parent nucleus.

In ref. [15], a single decay chain of $^{287}\text{115}$ was observed on increasing the projectile energy by 5 MeV to $E = 253$ MeV. It is assumed that $4n$ evaporation channel in the excitation function becomes dominant. It may, however, be said that any other event for this decay chain has not been observed to confirm the α -decay energies. In view of this, these values may be treated with caution. The

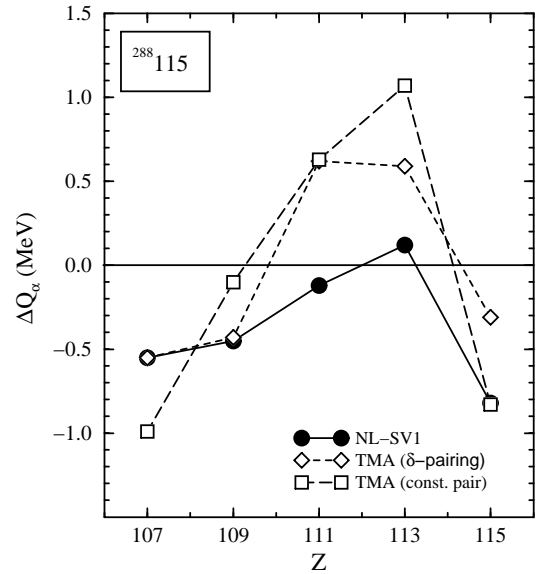


FIG. 1: The difference $\Delta Q_\alpha = Q_\alpha$ (theory) - Q_α (expt.) between the theoretical and the experimentally observed Q_α values for the α -decay chain with the parent nucleus $^{288}\text{115}$. The RMF results with NL-SV1 (full circles) are compared to those with the RMF calculations using the force TMA with constant pairing gap (open squares) and using a density-dependent δ -pairing force including blocking effect (open diamonds).

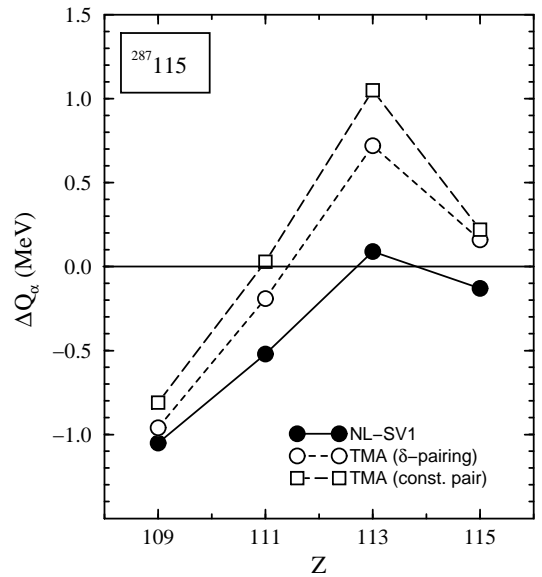


FIG. 2: The same as for Fig. 1, but for the α -decay chain with the parent nucleus $^{287}\text{115}$.

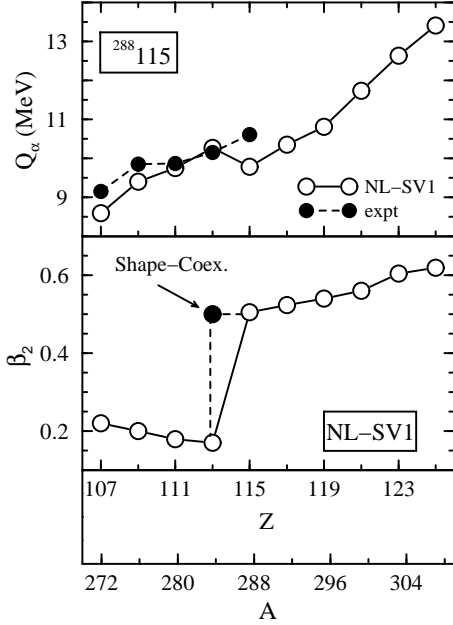


FIG. 3: The Q_α values obtained with the force NL-SV1 in the RMF calculations are compared with the experimental data from ref. [15] for the α -decay chain of $^{288}\text{115}$ in the upper panel. The Q_α values predicted by our model for the heavier parents of this chain are also shown. In the lower panel the ground-state quadrupole deformation β_2 are shown by open circles. The solid circle for the nucleus $^{284}\text{113}$ exhibits a second minimum at the highly deformed (superdeformed) configuration that is in coexistence with the low deformed prolate state.

α -decay energies for the decay chain of $^{287}\text{115}$ as reported in the ref. [15] are 10.59 MeV, 10.12 MeV, 10.37 MeV and 10.33 MeV, respectively. The two latter values show an increase over that of the second value (10.12 MeV) in the decay chain. This behaviour is different from that of the $^{287}\text{115}$ decay chain, where the α -decay energies show a decreasing trend with the decrease in the Z value of the daughter nuclei. Assuming that the shell structure has not changed from the $^{288}\text{115}$ chain to the $^{287}\text{115}$ chain, there could easily be an uncertainty of about 0.5 MeV in the α -decay energies of $^{279}\text{111}$ and $^{275}\text{109}$.

The results of our calculations for the decay chain of $^{287}\text{115}$ are shown in Fig. 2. The Q_α values with NL-SV1 agree well with the experimental values for the nuclei $^{287}\text{115}$ and $^{283}\text{113}$. For the nucleus $^{279}\text{111}$, our calculations show a Q_α of 10.0 MeV compared to 10.52 MeV as observed in ref. [15]. The difference is accentuated to about 1 MeV for the nucleus $^{275}\text{109}$. It is noted that the calculated values with NL-SV1 show a decreasing trend with the Z value. An uncertainty in the α -decay energies for this decay chain as commented above may partly account for this discrepancy. Generally, there is an overall

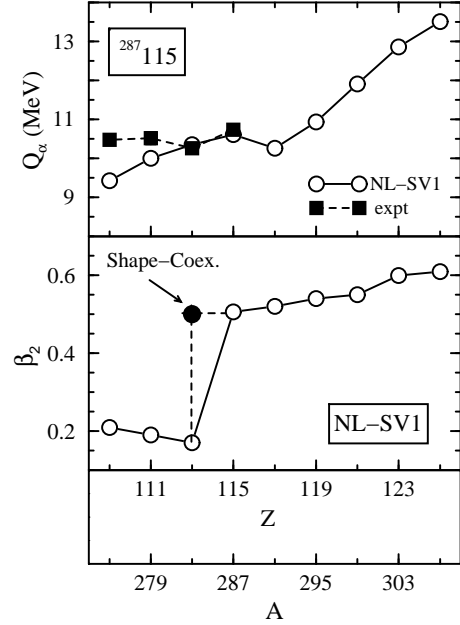


FIG. 4: The same as for Fig. 3 but for the chain consisting of the nucleus $^{287}\text{115}$.

agreement of the NL-SV1 results within 0.5 MeV for the Q_α values save that for ^{275}Mt ($Z = 109$).

Calculations with TMA from ref. [48] are also compared in Fig. 2. The calculations both with constant pairing and with δ -pairing with blocking show a trend similar to that of NL-SV1 vis-a-vis the experimental values. In the calculations of ref. [48] disagreements are more pronounced for $^{283}\text{113}$ and ^{275}Mt ($Z = 109$).

B. Predictions for heavier superheavy nuclei

We have calculated ground-state properties of the decay chains of ref. [15]. We have also extended our calculations in order to be able to predict properties of odd- Z nuclei heavier than $^{288}\text{115}$ and $^{287}\text{115}$, whereby $^{288}\text{115}$ and $^{287}\text{115}$ would constitute daughter nuclei of a sequential α -decay chain. The Q_α value and quadrupole deformation β_2 corresponding to the lowest energy state for the chain comprising the $^{288}\text{115}$ and its daughters are shown in Fig. 3. The NL-SV1 results show general agreement with the experimental Q_α values [15] (see Table II) as discussed above and shows an increasing trend with an increase in the Z value. The NL-SV1 value, on the other hand, shows a slight decrease at $Z = 115$. This is indicative of a possible deformed shell closure at $Z = 114$ with NL-SV1. For all the nuclei above $Z = 115$, the Q_α value shows a systematic increase with a slight kink at $Z = 119$.

The corresponding β_2 values are shown in the lower

TABLE II: The Q_α values, α -decay half-lives T_α , and quadrupole deformation β_2 of nuclei in the decay chain consisting of the nuclide $^{288}\text{115}$ as obtained with RMF calculations using the Lagrangian set NL-SV1. The Q_α values and estimated half-lives from the recent experimental results [15] are also shown for comparison.

Nucleus	Q_α (MeV)	T_α	β_2	Q_α (exp.) (MeV)	T_α (exp.)
$^{308}\text{125}$	13.41	$16\ \mu\text{s}$	0.62		
$^{304}\text{123}$	12.64	0.20 ms	0.61		
$^{300}\text{121}$	11.74	6.5 ms	0.56		
$^{296}\text{119}$	10.81	0.38 s	0.54		
$^{292}\text{117}$	10.35	1.63 s	0.52		
$^{288}\text{115}$	9.79	15.3 s	0.50	10.61 ± 0.06	$87^{+105}_{-30}\ \text{ms}$
$^{284}\text{113}$	10.27	0.15 s	0.17	10.15 ± 0.06	$0.48^{+0.58}_{-0.17}\ \text{s}$
$^{280}\text{111}$	9.75	0.97 s	0.18	9.87 ± 0.06	$3.6^{+4.3}_{-1.3}\ \text{s}$
^{276}Mt	9.40	2.21 s	0.20	9.85 ± 0.06	$0.72^{+0.87}_{-0.25}\ \text{s}$
^{272}Bh	8.60	150 s	0.26	9.15 ± 0.06	$9.8^{+11.7}_{-3.5}\ \text{s}$

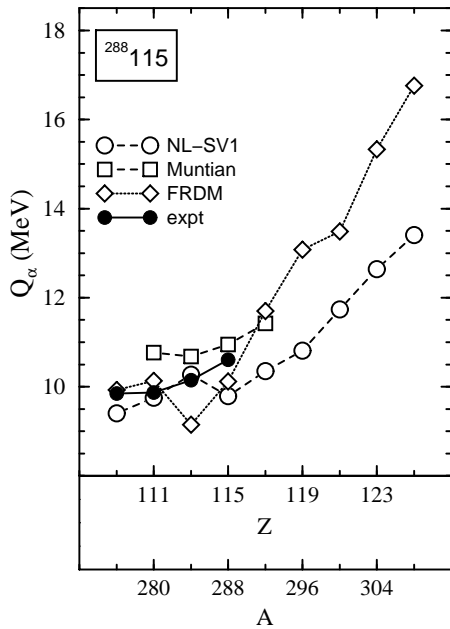


FIG. 5: A comparison of the Q_α values obtained with NL-SV1 is made with the results of ref. [22] and FRDM [52] for the chain comprising $^{288}\text{115}$. The experimental values obtained from the recent experiment [15] are also shown for comparison.

panel. The quadrupole deformation stays in the vicinity of $\beta_2 \sim 0.2$ in going from $Z = 107$ to $Z = 113$. However, the nucleus $^{284}\text{113}$ marks a transition point for the chain, in that it exhibits a shape coexistence of a low prolate deformation ($\beta_2 = 0.17$) with a high prolate deformation ($\beta_2 = 0.50$) in the ground state. Here, the state with the low deformation is the lowest one. All the nuclei including and above $Z = 115$ exhibit a large prolate deformation ($\beta_2 \sim 0.6$) in the ground state. This is akin to a superdeformation. As the single-particle scheme

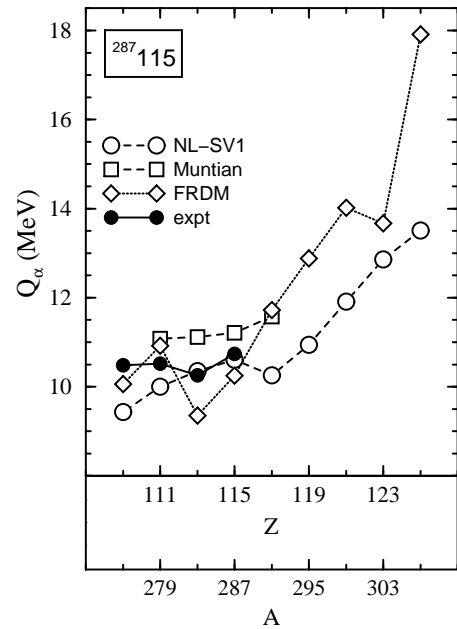


FIG. 6: The same as for Fig. 5 but for the chain consisting of the nuclide $^{287}\text{115}$.

would show, this is associated with a strong shell gap at $Z = 118$ in the superdeformed region. This allows an increase in the binding energies of nuclei and accordingly the Q_α values are comparatively suppressed.

The Q_α and β_2 values for the ground state of nuclei in the chain associated with $^{287}\text{115}$ are shown in Fig. 4. As discussed above, the Q_α value for the nucleus ^{275}Mt shows a deviation of about 1 MeV from the observed value. For the others, there is a good agreement with the experimental value (see Table III). The NL-SV1 values show a systematic increase in Q_α in going from $Z = 109$ to $Z = 115$. A kink in Q_α at $Z = 115$ indicates a presence of deformed shell closure at $Z = 114$.

TABLE III: The same as for Table II but for the decay chain consisting of the nuclide $^{287}\text{115}$.

Nucleus	Q_α (MeV)	T_α	β_2	Q_α (exp.) (MeV)	T_α (exp.)
$^{307}\text{125}$	13.51	10 μs	0.61		
$^{303}\text{123}$	12.86	68 μs	0.60		
$^{299}\text{121}$	11.91	2.6 ms	0.55		
$^{295}\text{119}$	10.94	0.17 s	0.54		
$^{291}\text{117}$	10.26	2.9 s	0.52		
$^{287}\text{115}$	10.57	100 ms	0.51	10.74 ± 0.06	32^{+155}_{-14} ms
$^{283}\text{113}$	10.35	90 ms	0.17	10.26 ± 0.06	100^{+490}_{-45} ms
$^{279}\text{111}$	10.00	200 ms	0.19	10.52 ± 0.06	170^{+810}_{-80} ms
^{275}Mt	9.43	1.8 s	0.21	10.48 ± 0.06	$9.7^{+46}_{-4.4}$ ms

As far as deformation of nuclei in this chain is concerned, all nuclei with low Z values including $^{283}\text{113}$ exhibit a low value of β_2 in the vicinity of 0.20. Here, the nucleus $^{283}\text{113}$ with $Z = 113$ exhibits the phenomenon of shape coexistence of a low prolate deformation ($\beta_2 = 0.17$) with a high prolate deformation ($\beta_2 = 0.50$) in the ground state. The state with the low β_2 value is the lowest minimum in the binding energy. This behavior is similar to that exhibited by the corresponding nucleus $^{284}\text{113}$ in the other chain. Likewise, the nucleus $^{283}\text{113}$ marks a transition point in the shapes of nuclei in this chain. All the nuclei including and above $Z = 115$ show a superdeformed ground state. All the features shown in Fig. 4 for this chain exhibit a similarity to those shown in Fig. 3. Therefore, properties of nuclei for both the chains point to almost the same structural behavior.

RMF calculations with another Lagrangian parameter set NL-SV2 [43, 45] with the vector self-coupling of ω -meson for both the chains of Figs. 3 and 4 show that nuclei $^{284}\text{113}$ and $^{283}\text{113}$ exhibit a shape coexistence of low prolate deformation with a high prolate deformation in the ground state. The magnitude of deformations with NL-SV2 is seen to be similar to that obtained with NL-SV1 as shown in Figs. 3 and 4. With the Lagrangian set NL-SV2, superheavy nuclei heavier than $^{284}\text{113}$ and $^{283}\text{113}$ in these chains are also observed to be superdeformed in the ground state. Accordingly, the nuclei $^{284}\text{113}$ and $^{283}\text{113}$ denote a transition point from a low deformation to a superdeformation also with NL-SV2. Thus, the results on the shape-coexistence and the presence of a second superdeformed minimum for nuclei with $Z = 113$ with NL-SV1 are also exhibited by NL-SV2. A comprehensive comparison of results in the superheavy region with various Lagragian models will be presented elsewhere [50].

In a recent investigation of deformation properties of superheavy nuclei [51], it has been noted that macroscopic-microscopic approach does not support a superdeformation in the superheavy region. This difference in the outcome of the results of ref. [51] can be understood due to strong shell effects prevalent in the macroscopic-microscopic approaches. The strong shell effects or equivalently strong shell gaps would disfavour a superdeformation.

Our results for the recently discovered chain of $^{288}\text{115}$ and predictions for heavier superheavy nuclei are compared with some other models in Fig. 5. Detailed macroscopic-microscopic calculations for a large number of nuclei in the superheavy region of $Z = 110 - 120$ have recently been performed by Muntian et al. [22]. The results available on some nuclei in this chain are shown. Whilst this model shows a reasonably good agreement with the experimental values on $^{288}\text{115}$ and $^{284}\text{113}$, it overestimates the datum for $^{280}\text{111}$. It is interesting to compare the data also with those from the macroscopic-microscopic model FRDM [52]. The FRDM values show an agreement with the data for two lighter superheavy nuclei and also for $^{288}\text{115}$ within about 0.5 MeV. However, for the nucleus $^{284}\text{113}$ the FRDM value underestimates the Q_α value by ~ 1 MeV. For heavier α -decay precursors of $^{288}\text{115}$, i.e., nuclei with $Z = 117 - 125$, we can compare our results with NL-SV1 with those from FRDM.

As far as a comparison of the macroscopic-microscopic calculations of Muntian et al. [22] with FRDM are concerned, the predictions only for $^{292}\text{117}$ can be compared. For this nucleus the two models agree. As further results on other odd nuclei from ref. [22] are not available, it is difficult to compare the two models in the context of the two chains studied in our work. However, as predictions from ref. [22] are generally on the higher side in this region, we surmise that the results of the two macroscopic-microscopic would follow each other for heavier superheavies. In comparison, our results with NL-SV1 show a smooth increase in the value of Q_α with Z value. The NL-SV1 results, on the other hand, predict Q_α values which are smaller by about 1-2 MeV from those of the FRDM. This is due to an extra stability lent by the superdeformed ground state of all the heavier nuclei with $Z \geq 115$. This will be demonstrated by a large shell gap in the deformed single-particle spectrum at $Z = 118$ and $Z = 120$.

Calculation of half-lives of α -decay from Q_α values is not free of uncertainties. This is subject to Viola-Seaborg systematics fitted over a given region of nuclei. The mostly used systematics derive from a fit of parameters done in ref. [53]. We have calculated the α -decay half-lives of nuclei using the formula from Viola-Seaborg

systematics. Accordingly, the α -decay half-life can be written as

$$\log T_\alpha(s) = (aZ + b)Q_\alpha^{-1/2} + (cZ + d) \quad (4)$$

where Z is proton number and Q_α is alpha-decay energy of the parent nucleus in MeV. The parameters are $a = 1.66175$, $b = -8.5166$, $c = -0.20228$ and $d = -33.9069$. These parameters are taken from ref. [53], where these were readjusted in order to take into account new data. These parameters have been found to be successful over a broad range of nuclei.

The T_α values calculated using Q_α values from NL-SV1 for nuclei of the chain consisting of $^{288}115$ are shown in Table II. The experimentally observed α -decay half-life [15] of $^{288}115$ and its daughters are also shown for comparison. It may be noted that experimental values of T_α for this chain are based upon 3 events observed in the experiment [15]. The corresponding half-life quoted in ref. [15] has been obtained from the average of the life-times observed in the experiment. Consequently, one can notice large error bars in the experimental values. These values therefore signify the order of magnitude of a T_α value.

Given the large uncertainties in the experimental values, T_α values calculated with NL-SV1 agree well with the experimental ones with the exception for $^{288}115$ and ^{272}Bh (see Table II). The theoretical half-life for these two nuclei are about an order of magnitude larger than the experimental values. This is due to the reason that with our model the Q_α values are $\sim 0.50 - 0.80$ MeV smaller than the experimental Q_α value. For other superheavy nuclei with $Z = 109 - 113$, there is a good agreement between the theoretical and experimental α -decay half-lives. This is due to a good agreement between the corresponding Q_α values.

In going to the heavier precursor nuclei in the same chain (Table II), there is an increasing tendency in the value of Q_α with an increase in the Z value. However, Q_α values with NL-SV1 are systematically lower than those of FRDM. The lower Q_α values with NL-SV1 has the consequence that superheavy nuclei with high Z such as $Z = 117$, $Z = 119$ and $Z = 121$ would not have a very small α -decay half-life as compared to that from FRDM. The α -decay half-lives predicted from NL-SV1 for the nuclei $^{292}117$, $^{296}119$, and $^{300}121$ are ~ 1.6 s, 0.4 s and 7 ms, respectively. This would put these nuclei within the range of experimental accessibility and feasibility.

A comparison of various results for the chain comprising $^{287}115$ are shown in Fig. 6. In general, the results of Muntian et al. [22] overestimate the new data by ~ 0.5 - 1.0 MeV. On the other hand, the results of FRDM for this chain are very similar to those for the other chain as shown in Fig. 5. Though the FRDM results show a good agreement with a few data, kinks at $Z = 111$ and $Z = 113$ show an undulating character of the FRDM results. Such kinks are not present in other results. This may be due to a strong spherical shell closure at $Z = 114$ as predicted by the FRDM.

The α -decay half-lives for the decay chain of $^{287}115$ from NL-SV1 are compared with the experimental estimates from ref. [15] in Table III. It may be noted that the experimental value is based upon life-time estimates from a single decay event of the superheavy nucleus $^{287}115$. There is an overall good agreement between NL-SV1 values and the experimental ones. Only for ^{275}Mt ($Z = 109$) does NL-SV1 overestimate the half-life by about 2 orders of magnitude. The experimental half-life for the nucleus ^{275}Mt has been estimated to be $9.7^{+46}_{-4.4}\text{ms}$. This value is much lower than the experimental estimates for the heavier superheavies such as $^{279}111$ and $^{283}113$ (see Table III). In comparison, the experimental Q_α value for ^{275}Mt is comparable to that for $^{279}111$. According to Viola-Seaborg formula, this experimental Q_α for ^{275}Mt would indicate T_α value much larger than the quoted one [15]. In view of this, there seems to be a little discrepancy between the experimentally deduced Q_α and T_α value for the nucleus ^{275}Mt . This may be due to ambiguities in identification in a single event.

The generally higher Q_α values from macroscopic-microscopic calculations [22] vis-a-vis the experimental data [15] by $\sim 0.5 - 1.0$ MeV would mean a decrease in α -decay half-life by about 1-3 orders of magnitude in the macroscopic-microscopic calculations [22]. However, it is worth mentioning that the results of ref. [22] on α -decay energies describe well the data on and variation in the Q_α values with neutron numbers for isotopic chains below $Z = 109$, as shown clearly in Fig. 2 of ref. [15].

For the heavier superheavies of the chain comprising of the nucleus $^{287}115$ (Fig. 6) the FRDM values show a strong increase in the Q_α value. This would make the half-life of some of these nuclei in the range of nanosecond or even smaller. In comparison, our predictions with NL-SV1 show only a modest increase in the Q_α values for nuclei heavier than $Z = 115$ (see Table III). This behaviour is very similar to that exhibited by the other chain in Fig. 5. The α -decay half-life using the Viola-Seaborg systematics for nuclei $^{292}117$, $^{296}119$, and $^{300}121$ in our model are 2.9 s, 0.17 s and 2.6 ms, respectively. These values are well within the reach of experimental feasibility. Thus, the NL-SV1 results shown in Fig. 5 and Fig. 6 puts several heavy elements within the range of feasibility of realization.

C. Potential energy landscapes

We have performed constrained calculations with a quadratic constraint in order to map out potential energy landscape. The total energy of nuclei as a function of quadrupole deformation β_2 is shown in Figs. 7 and 8 for superheavy nuclei in the two isotopic chains studied in this work. All the nuclei of chain comprising of both $^{288}115$ (Fig. 7) and $^{288}115$ (Fig. 8) exhibit a prolate deformation for all the nuclei from $Z = 111$ to $Z = 125$. A configuration in oblate space seems to be forbidden as suggested by the total potential energy curve for the

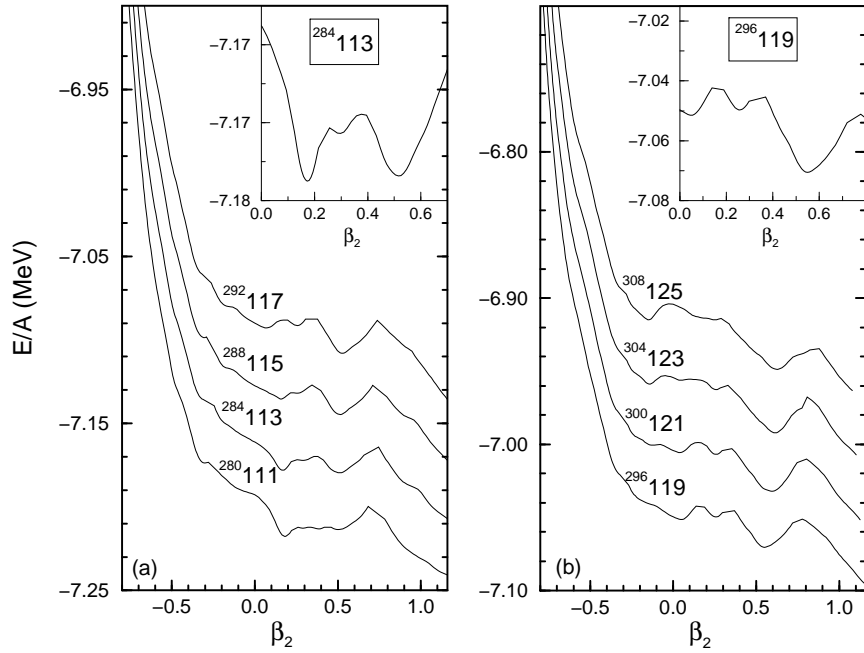


FIG. 7: Potential energy landscapes of nuclei in the decay chain comprising $^{288}115$ for (a) lighter superheavies below $Z \leq 117$. The shape coexistence of a deformed and a superdeformed prolate shape is shown for $^{283}113$ in the inset. (b) Potential energy landscapes of heavy superheavies with $Z \geq 119$. All the nuclei show a superdeformed ground state as depicted in the inset for $^{296}119$.

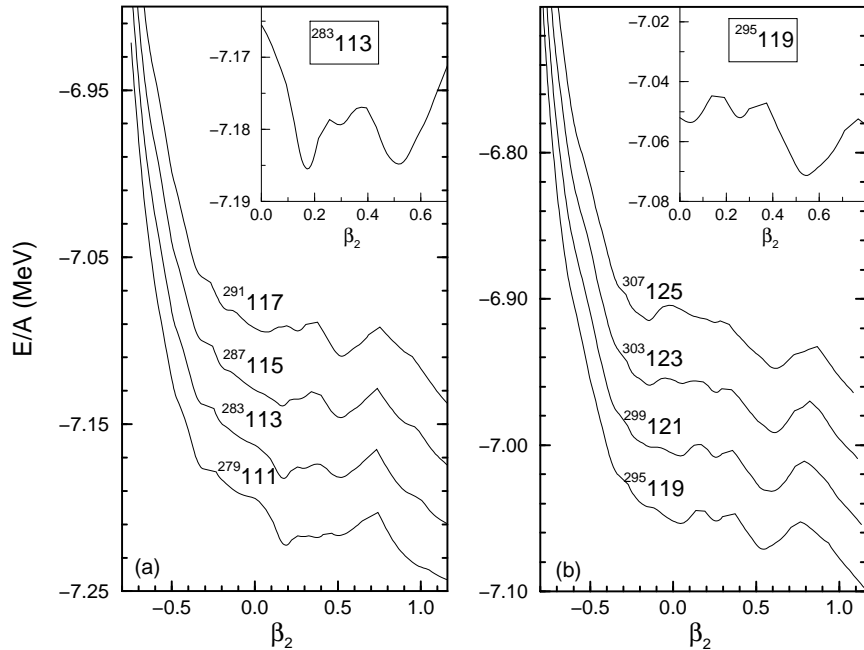


FIG. 8: The same as for Fig. 7, but for the decay chain comprising of the nuclide $^{287}115$.

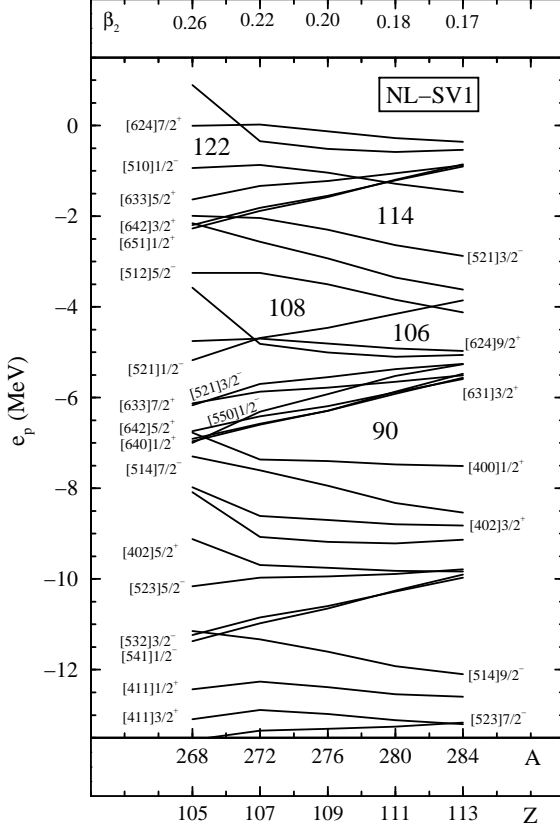


FIG. 9: The proton Nilsson single-particle levels obtained from the RMF calculations with NL-SV1 for low-deformed prolate-shaped nuclei of the decay chain of $^{288}\text{115}$ are shown.

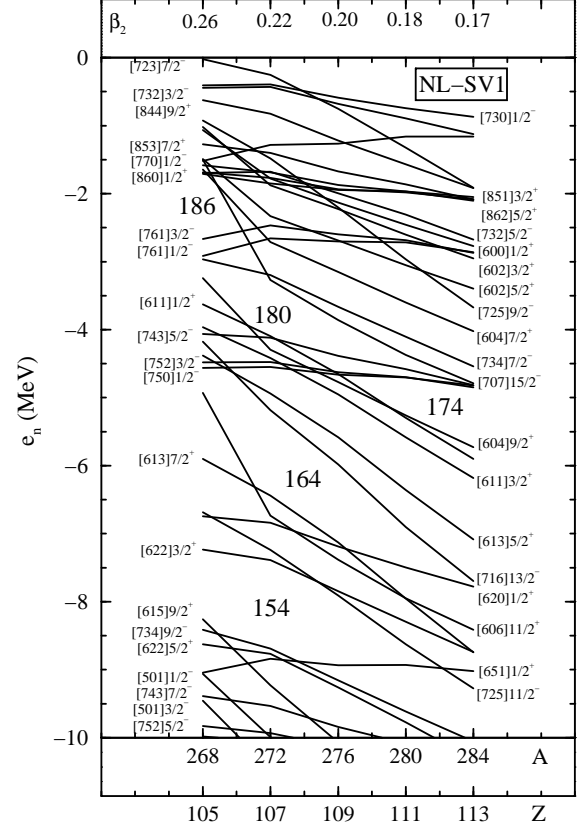


FIG. 10: The neutron Nilsson single-particle levels obtained from the RMF calculations with NL-SV1 for low-deformed prolate-shaped nuclei of the decay chain of $^{288}\text{115}$ are shown.

superheavy nuclei shown in Figs. 7 and 8.

Consistent with previous description, the nuclei $^{280}\text{111}$ and $^{279}\text{111}$ are prolate deformed with a low value of quadrupole deformation. On the other hand, the nuclei $^{284}\text{113}$ (Fig. 7(a)) and $^{283}\text{113}$ (Fig. 8(a)) exhibit two minima, as discussed earlier. The two minima, which co-exist in energy are depicted in the insets of Fig. 7(a) and Fig. 8(a). The second minimum at $\beta_2 \sim 0.50$ lies within a few hundred keV of the first minimum. For all the heavier elements with $Z > 113$, the ground state minimum is obtained in the region of a high prolate deformation as seen by a single well in the curves in part (a) and (b) of Figs. 7 and 8. The high prolate deformation of superheavies continues in the high Z region as exemplified in the insets of Fig. 7(b) and Fig. 8(b) for the element $Z = 119$. It is interesting to note that the potential energy landscapes for Fig. 7 are very similar to those of Fig. 8.

D. Single-particle levels

The Nilsson single-particle levels obtained with NL-SV1 for the nuclei of chain $^{288}\text{115}$ are shown in Figs. 9 and 10. The proton single-particle levels for nuclei in this chain are presented in Fig. 9. The corresponding ground-state β_2 values for each nucleus are indicated in the top panel of the figure. It shows a decrease from 0.26 to 0.17 in going from ^{268}Db ($Z = 109$) to $^{284}\text{113}$. This decrease is accompanied by an arrival of a deformed shell gap at $Z = 114$ as seen in the figure. There are also minor deformed shell gaps at $Z = 106$ and $Z = 108$. As the deformation is changing only slightly and the Fermi energy is showing a marginal change in going from the left to the right, the level crossing in Fig. 9 is not such a dominant feature. However, shifting of the deformed levels partly due to the change in deformation and partly due to the change in the chemical potential, deformed shell gaps are being created at $Z = 108$ for the lower Z nuclei and at $Z = 114$ for the higher Z nuclei. There is, however, no spherical $Z = 114$ closed shell as suggested in models such as FRDM [19].

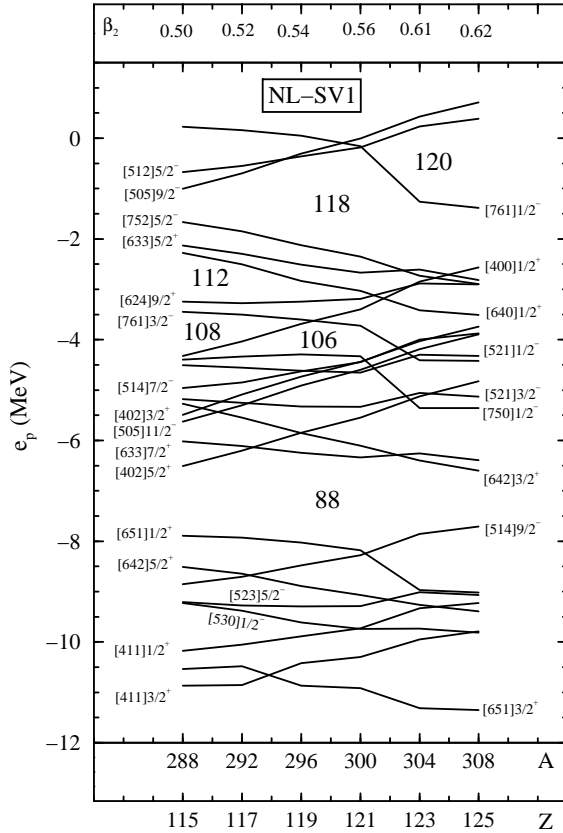


FIG. 11: The proton Nilsson single-particle levels obtained from RMF calculations with NL-SV1 for superdeformed prolate nuclei, which are α -decay precursors of the nucleus $^{288}\text{115}$.

The neutron single-particle levels in Fig. 10 show a shell gap at $N = 154$ and $N = 164$. The latter is inevitably associated with the nuclei ^{268}Db and ^{272}Bh . For the heavier nuclei with $A = 280$ and $A = 284$ the deformed shell gap evolves at $N = 174$. This has been observed to the case in several other models. It can be seen that a frequent crossing of levels creates a bunching and thus deformed shell gaps at $N = 154$, $N = 164$, $N = 174$ and $N = 180$ are produced. The well-known shell gap at $N = 184$ is not seen in this figure, though it is not relevant to mass numbers shown in this figure.

The proton Nilsson orbitals for the precursors of the nucleus $^{288}\text{115}$ are shown in Fig. 11. For these nuclei the ground state quadrupole deformation β_2 increases from 0.50 for $^{288}\text{115}$ to 0.62 for $^{308}\text{125}$. Because these nuclei are superdeformed, there is a significant level crossing in this diagram. A deformed shell gap at $Z = 112$ is seen. However, this shell gap is much less relevant to the higher Z values of nuclei considered in this figure. For the experimentally observed nucleus $^{288}\text{115}$ [15], there is no perceptible observation of a deformed shell gap at $Z = 114$. This gap which was seen in the lighter counterparts

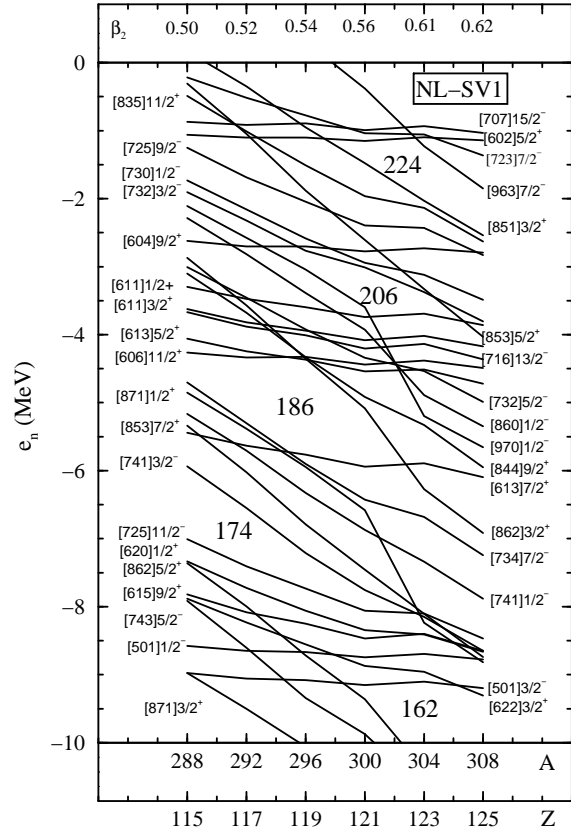


FIG. 12: The neutron Nilsson single-particle levels obtained from RMF calculations with NL-SV1 for superdeformed prolate nuclei, which are α -decay precursors of the nucleus ^{288}Nb .

of the chain is washed out here. In contrast, a strong shell gap is observed at $Z = 118$. This shell gap in the highly deformed region provides an extra stability to the nuclei concerned. This has already been seen in terms of lower Q_α values for nuclei with higher Z as shown in Fig. 5. A possible deformed shell closure at $Z = 120$ is also observed, but for very heavy superheavies. Here the nuclide $^{308}125$ runs close to the proton drip line.

The corresponding neutron Nilsson orbitals for the superdeformed superheavy nuclei which are heavier parents of the nucleus $^{288}\text{115}$ are shown in Fig. 12. The neutron number for these nuclei spans the range $N = 173 - 183$. For the lighter counterparts of the chain one can see a deformed shell gap at $N = 174$, that diminishes in going to the heavier nuclei. There is another deformed shell gap at $N = 186$. However, we do not see a shell gap at $N = 184$ in the deformed region. Moreover, nuclei in the vicinity of this neutron number are assuming superdeformed prolate shapes. This discounts the possibility of a deformed shell gap at $N = 184$ for these Z values. For Z values much lower than those considered in this work, a spherical shell gap at $N = 184$ can not be ruled out

within this model. Comprehensive calculations for much of the superdeformed region with this model in future would clarify the situation.

A lowering in energy of a large number of Nilsson orbitals in going from $^{288}115$ to $^{300}121$ is accompanied by a slight increase in the quadrupole deformation. However, splitting of levels by the strong deformation leads to a significant increase in the binding energy of nuclei. A sudden jump in the β_2 value from the nucleus $^{300}121$ to $^{304}123$ also results in a kink in several levels and a further lowering in the energy of several Nilsson orbitals is anticipated. Therefore, this adds to the total binding energy of nuclei such as $^{304}123$ and $^{308}125$. The consequence of this has already been seen in Figs. 5 and 6, where the Q_α value of heavier superheavies is smaller by $\sim 1\text{-}2$ MeV as compared to FRDM. This would inevitably provide a larger stability and consequently a larger α -decay half-lives as compared to the FRDM. Thus, the present calculations with NL-SV1 present an optimistic picture for producing superheavy nuclei heavier than $Z = 115$.

E. Shell effects in nuclei and consequences

As mentioned in Section I, the spin-orbit interaction and consequently its effect on the shell gaps and shell effects has a major influence on creation of magic numbers. It is, however, still not clear as to how the spin-orbit interaction extrapolates in the extreme limits of the periodic table such as near the r-process path and for extreme superheavy nuclei. We believe that both these regions have a bearing upon each other. Inevitably, how the shell effects would transcend and extrapolate in unknown regions would be decisive in r-process nucleosynthesis of heavy nuclei as well as in synthesis of extreme superheavy nuclei. We put up the case in Section II that if the shell effects are strong along the line of stability, these would extrapolate strongly in the extreme regions and vice-versa. This was demonstrated reasonably well in ref. [44].

Here a comment on the strength of the shell effects would be in order. It is well known that the macroscopic-microscopic approaches such as FRDM [52] exhibit shell effects that are stronger at $N = 82$ and $N = 132$ in going to extremely rich regions of the r-process path. The strong shell effects at these magic numbers in FRDM has a consequence on the r-process nuclear abundances. Using the data from the FRDM in network chain calculations, there is a considerable shortfall (troughs) in the abundance of r-process nucleosynthesis of nuclei below the peaks at $A \sim 130$ and $A \sim 190$ [54]. These peaks in the abundance curve correspond to the above neutron magic numbers. Therefore, the strong shell effects in FRDM are not consistent with the r-process nuclear abundances which require a weakening of the shell effects in going to the r-process region. The strong nature of the shell effects in the FRDM is evidently carried away also in the region of superheavy nuclei. This becomes appar-

ent in going to extreme superheavies in the neighborhood of $Z = 120$ as shown in Fig. 5 and 6, where large values of Q_α are predicted by the FRDM.

The macroscopic-microscopic calculations of ref. [22] are of the similar origin as the FRDM. These calculations have been successful in describing superheavy nuclei below $Z = 109$ as illustrated in Fig. 2 of ref. [15]. As mentioned earlier, results of ref. [22] overestimate the Q_α values (see Fig. 5 and 6) for superheavy nuclei above $Z = 111$ [15]. However, comparing the general trend of the predictions from macroscopic-microscopic calculations of ref. [22] with those of the FRDM near $Z = 120$, one finds a reasonably good agreement between the two model predictions on Q_α values. Both the models predict larger values for Q_α in the extreme region. This suggests that similar to the FRDM, strong shell effects are also carried over to the extreme region in the calculations of ref. [22]. This would indeed lead to very small α -decay half-lives for very heavy superheavy nuclei. On the other hand, the less strong shell effects in microscopic calculations with NL-SV1 predict Q_α values that are smaller than those of the FRDM. This shows an immense importance of as to how the shell effects extrapolate in the extreme regions and how the shell effects influence properties of nuclei in these regions.

VI. CONCLUSION

We have performed relativistic mean-field calculations for the recently observed alpha-decay chains of nuclei $^{288}115$ and $^{287}115$ using the Lagrangian set NL-SV1 with the vector self-coupling of ω -meson. The Q_α values have been calculated. It is shown that across the experimentally observed chains, the NL-SV1 values show a rather smooth behaviour with the change in the Z values of the nuclei. The Q_α values obtained with NL-SV1 without blocking of odd-particle pairing describe much of the experimental data very well. In comparison, the macroscopic-microscopic calculations [22] overestimate the experimental values systematically. The α -decay half-lives calculated with Q_α values from NL-SV1 using the Viola-Seaborg systematics show a reasonably good agreement with the experimental values deduced from the recent experiment [15] with the exception of a few nuclei.

The decay products of the both the chains with $Z = 107, 109, 111$ and 113 are shown to be prolate deformed with a deformation varying from $\beta_2 \sim 0.22$ for $Z = 107$ to $\beta_2 \sim 0.17$ for $Z = 113$. Curiously, the nuclei $^{284}113$ and $^{283}113$ in both the chains exhibit a shape-coexistence of a low prolate shape with $\beta_2 \sim 0.17$ and a superdeformed prolate shape with $\beta_2 \sim 0.50$. In both the cases, the low β_2 shape corresponds to the lowest energy minimum. The parent nuclei $^{288}115$ and $^{287}115$ of both the chains, however, exhibit a very large deformation akin to a superdeformed shape.

We have also made predictions for heavier elements in

the two chains of $^{288}\text{115}$ and $^{287}\text{115}$. It is shown that with NL-SV1 the ground-state of the higher Z counterparts of both the chains are superdeformed with β_2 values in the vicinity of 0.60 with a tendency of an increase in β_2 value in going to heavier elements. This can be attributed to a softening of the shell effects in going to the extreme case. The Q_α values obtained with NL-SV1 for nuclei with $Z = 117, 119, 121, 123$ and 125 are about 1-2 MeV lower than the predictions of the FRDM [19]. This has a consequence that α -decay half-lives of the heavier nuclei are 2-3 orders of magnitude larger than the existing predictions of very short half-lives from the macroscopic-

microscopic models [22, 52]. This scenario would put synthesis of heavier superheavy elements on a feasible footing.

Acknowledgments

This work is supported by the Research Administration Project No. SP05/02 of Kuwait University. We thank Professor Y.K. Gambhir for useful comments and discussion.

[1] S. Hofmann and G. Münzenberg, Rev. Mod. Phys. **72**, 733 (2000).

[2] S. Hofmann, V. Ninov, F.P. Hessberger, P. Armbruster, H. Folger, G. Münzenberg, H.J. Schött, A.G. Popeko, A.V. Yeremin, S. Saro, R. Janik, and M., Leino, Z. Phys. A **354**, 229 (1996).

[3] S. Hofmann, F.P. Hessberger, D. Ackermann, G. Münzenberg, S. Antalic, P. Cagarda, B. Kindler, J. Kojuharova, M. Leino, B. Lommel, R. Mann, A.G. Popeko, S. Reshitko, S. Saro, J. Uusitalo, and A.V. Jeremin, Eur. Phys. J. A **14**, 147 (2002).

[4] T.N. Ginter, K.E. Gregorich, W. Loveland, D.M. Lee, U.W. Kirbach, R. Sudowe, C.M. Folden III, J.B. Patin, N. Seward, P.A. Wilk, P.M. Zielinski, K. Aleklett, R. Eichler, H. Nitsche, and D.C. Hofmann, Phys. Rev. C **67**, 064609 (2003).

[5] K. Morita, M. Morimoto, D. Kaji, S. Goto, H. Haba, E. Ideguchi, R. Kanungo, K. Katori, H. Koura, H. Kudo, T. Ohnishi, A. Ozawa, J.C. Peter, T. Suda, K. Sueki, I. Tanihata, F. Tokanai, H. Xu, A. V. Yeremin, A. Yoneda, A. Yoshida, Y.-L. Zhao, and T. Zheng, AIP Conf. Proc., Tours Symposium on Nuclear Physics 2003, p. 13.

[6] K. Morita, K. Morimoto, D. Kaji, T. Akiyama, S. Goto, H. Haba, E. Ideguchi, K. Katori, H. Koura, H. Kudo, T. Ohnishi, A. Ozawa, T. Suda, K. Sueki, A. Yoneda, and A. Yoshida, Proc. Int. Symposium on Exotic Nuclei "Exon - 2004", Peterhof, Russia, July 2004, in preparation.

[7] G. Münzenberg, Rep. Prog. Phys. **51**, 57 (1988).

[8] P. Möller, J.R. Nix, W.D. Myers, and W.J. Swiatecki, At. Data Nucl. Data Tables **59**, 185 (1995).

[9] S. Cwiok, V. Pashkevich, J. Dudek, and W. Nazarewicz, Nucl. Phys. A**410**, 254 (1983).

[10] K. Böning, Z. Patyk, A. Sobiczewski, and S. Cwiok, Z. Phys. A **325**, 479 (1986).

[11] Yu.Ts. Oganessian, V.K. Utyonkov, Yu.A. Lobanov, F.Sh. Abdullin, A.N. Polyakov, I.V. Shirokovski, Yu.S. Tsyanov, G.G. Gulbekian, S.L. Bogomolov, B.N. Gikal, A.N. Mezentsev, S. Iliev, V.G. Subbotin, A.M. Sukhov, G.V. Buklanov, K. Subotic, M.G. Itkis, K.J. Moody, J.F. Wild, N.J. Stoyer, M. A. Stoyer, and R.W. Lougheed, Phys. Rev. Lett. **83**, 3154 (1999).

[12] Yu.Ts. Oganessian, V.K. Utyonkov, Yu.A. Lobanov, F.Sh. Abdullin, A.N. Polyakov, I.V. Shirokovski, Yu.S. Tsyanov, G.G. Gulbekian, S.L. Bogomolov, B.N. Gikal, A.N. Mezentsev, S. Iliev, V.G. Subbotin, A.M. Sukhov, O.V. Ivanov, G.V. Buklanov, K. Subotic, M.G. Itkis, K.J. Moody, J.F. Wild, N.J. Stoyer, M.A. Stoyer, R.W. Lougheed, C.A. Laue, Ye.E. Karelina, and A.N. Tatarinov, Phys. Rev. C **63**, 011301 (R) (2000).

[13] Yu.Ts. Oganessian, V.K. Utyonkov, Yu.A. Lobanov, F.Sh. Abdullin, A.N. Polyakov, I. V. Shirokovski, Yu.S. Tsyanov, G.G. Gulbekian, S.L. Bogomolov, B.N. Gikal, A.N. Mezentsev, S. Iliev, V.G. Subbotin, A.M. Sukhov, O.V. Ivanov, G.V. Buklanov, K. Subotic, V.I. Zagrebaev, M.G. Itkis, J. B. Patin, K.J. Moody, J.F. Wild, M.A. Stoyer, N.J. Stoyer, D.A. Shaughnessy, J.M. Kennally, and R.W. Lougheed, Phys. Rev. C **69**, 054607 (2004).

[14] Yu.Ts. Oganessian, V.K. Utyonkov, Yu.A. Lobanov, F.Sh. Abdullin, A.N. Polyakov, I. V. Shirokovski, Yu.S. Tsyanov, G.G. Gulbekian, S.L. Bogomolov, B.N. Gikal, A.N. Mezentsev, S. Iliev, V.G. Subbotin, A.M. Sukhov, A.A. Voinov, G.V. Buklanov, K. Subotic, V.I. Zagrebaev, M.G. Itkis, J.B. Patin, K.J. Moody, J.F. Wild, M.A. Stoyer, N.J. Stoyer, D.A. Shaughnessy, J.M. Kenneally, and R.W. Lougheed, Phys. Rev. C **69**, 021601 (R) (2004).

[15] Yu.Ts. Oganessian, V.K. Utyonkov, Yu.V. Lobanov, F. Sh. Abdullin, A. N. Polyakov, I. V. Shirokovsky, Yu.S. Tsyanov, G.G. Gulbekian, S.L. Bogomolov, A.N. Mezentsev, S. Iliev, V.G. Subbotin, A.M. Sukhov, A.A. Voinov, G.V. Buklanov, K. Subotic, V.I. Zagrebaev, M.G. Itkis, J.B. Patin, K.J. Moody, J.F. Wild, M.A. Stoyer, N.J. Stoyer, D.A. Shaughnessy, J.M. Kenneally, and R.W. Lougheed, Phys. Rev. C **69**, 021601 (R) (2004).

[16] A. Tuerler, Proc. Int. Symposium on Exotic Nuclei "Exon - 2004", Peterhof, Russia, July 2004, in preparation.

[17] V.M. Strutinsky, Nucl. Phys. **A95**, 420 (1967).

[18] V.M. Strutinsky, Nucl. Phys. **A122**, 1 (1968).

[19] P. Möller, J.R. Nix, W.D. Myers and W.J. Swiatecki, At. Data Nucl. Data Tables **59**, 185 (1995).

[20] A. Sobiczewski, I. Muntian, and Z. Patyk, Phys. Rev. C **63**, 034306 (2001).

[21] I. Muntian, Z. Patyk, and A. Sobiczewski, Acta. Phys. Pol. **32**, 691 (2001).

[22] I. Muntian, S. Hoffman, Z. Patyk, and A. Sobiczewski, Acta. Phys. Pol. **34**, 2073 (2003).

[23] I. Muntian, Z. Patyk, and A. Sobiczewski, Phys. At. Nuclei **66**, 1015 (2003).

[24] S. Cwiok, J. Dobaczewski, P.-H. Heenen, P. Magierski, and W. Nazarewicz, Nucl. Phys. **A611**, 211 (1996).

[25] K. Rutz, M. Bender, T. Bürvenich, T. Schilling, P.-G. Reinhard, J.A. Maruhn, and W. Greiner, Phys. Rev. C **56**, 238 (1997).

[26] M. Bender, K. Rutz, P.-G. Reinhard, J.A. Maruhn, and

W. Greiner, Phys. Rev. C **60**, 034304 (1999).

[27] M. Bender, W. Nazarewicz, and P.-G. Reinhard, Phys. Lett. **B515**, 42 (2001).

[28] P.-G. Reinhard, M. Bender, and J.A. Maruhn, Comments on Mod. Phys. **2**, A177 (2002).

[29] M. Bender, P.-H. Heenen, and P.G. Reinhard Rev. Mod. Phys. **75**, 121 (2003).

[30] G.A. Lalazissis, M.M. Sharma, P. Ring, and Y.K. Gambhir, Nucl. Phys. **A608**, 202 (1996).

[31] M.M. Sharma, M.A. Nagarajan, and P. Ring, Phys. Lett. **B312**, 377 (1993).

[32] A.T. Kruppa, M. Bender, W. Nazarewicz, P.-G. Reinhard, T. Vertse, and S. Cwiok, Phys. Rev. C **61**, 034313 (2004).

[33] M.M. Sharma, G.A. Lalazissis, J. König, and P. Ring, Phys. Rev. Lett. **74**, 3744 (1994).

[34] P.-G. Reinhard and H. Flocard, Nucl. Phys. **A584**, 467 (1995).

[35] T. Bürvenich, M. Bender, J.A. Maruhn, and P.-G. Reinhard, Phys. Rev. C **69**, 14307 (2004).

[36] B.D. Serot and J.D. Walecka, Adv. Nucl. Phys. **16**, 1 (1986).

[37] P.G. Reinhard, Rep. Prog. Phys. **52**, 439 (1989).

[38] Y.K. Gambhir, P. Ring, and A. Thimet, Ann. Phys. (N.Y.) **198**, 132 (1990).

[39] B.D. Serot, Rep. Prog. Phys. **55**, 1855 (1992).

[40] P. Ring, Prog. Part. Nucl. Phys. **37**, 193 (1996).

[41] B.D. Serot and J.D. Walecka, Mod. Phys. **E6**, 515 (1997).

[42] M. M. Sharma, G. A. Lalazissis, and P. Ring, Phys. Lett. B **317**, 9 (1993).

[43] M.M. Sharma and A.R. Farhan and S. Mythili, Phys. Rev. C **61**, 054306 (2000).

[44] M.M. Sharma and A.R. Farhan, Phys. Rev. C **65**, 044301 (2002).

[45] M.M. Sharma, in preparation (2005).

[46] A.R. Bodmer, Nucl. Phys. **A526**, 703 (1991).

[47] P. Möller, J.R. Nix, Nucl. Phys. **A536**, 221 (1992).

[48] L.S. Geng, H. Toki, and J. Meng, Phys. Rev. C **68**, 061303 (2003).

[49] Y. Sugahara and H. Toki, Nucl. Phys. **A579**, 557 (1994).

[50] A.R. Farhan, A. Anil and M.M. Sharma, in preparation (2005).

[51] I. Muntian and and A. Sobiczewski, Phys. Lett. B **586**, 254 (2004).

[52] P. Möller, J.R. Nix and K.L. Kratz, At. Data Nucl. Data Tables **66**, 131 (1997).

[53] A. Sobiczewski, Z. Patyk, and S. Cwiok, Phys. Lett. B **224**, 1 (1989).

[54] K.L. Kratz, J.P. Bitouzet, F.K. Thielemann, P. Möller, and B. Pfeiffer, Astrophys. J. **403**, 216 (1993).